

The interaction between the magnetic and superconducting order parameters in a $\text{La}_{1.94}\text{Sr}_{0.06}\text{CuO}_4$ wire

Meni Shay,¹ Amit Keren,¹ Gad Koren,¹ Amit Kanigel,¹ Oren Shalita,¹ Lital Marcipar,¹ Gerard Nieuwenhuys,² Elvezio Morenzoni,² Andreas Suter,² Thomas Prokscha,² Moshe Dubman,^{2,3} and Daniel Podolsky⁴

¹Department of Physics, Technion – Israel Institute of Technology, Haifa 32000, Israel

²Paul Scherrer Institute, CH 5232 Villigen PSI, Switzerland

³Institut für Physik der Kondensierten Materie, TU Braunschweig, D-38106 Braunschweig, Germany

⁴Department of Physics, University of Toronto, Toronto, Ontario, Canada M5S 1A7

(dated: February 21, 2024)

We investigate the coupling between the magnetic and superconducting order parameters in an 8 m long meander line ("wire") made of a $\text{La}_{1.94}\text{Sr}_{0.06}\text{CuO}_4$ film with a cross section of $0.5 \times 100 \text{ nm}^2$. The magnetic order parameter is determined using the Low-Energy muon spin relaxation technique. The superconducting order parameter is characterized by transport measurements and modulated by high current density. We find that when the superconducting order parameter is suppressed by the current, the magnetic transition temperature, T_m , increases. The extracted sign and magnitude of the Ginzburg-Landau coupling constant indicate that the two orders are repulsive, and that our system is located close to the border between first and second order phase transition.

When cuprates are doped their low temperature ordered phase changes from an antiferromagnetic (AFM) to a superconducting (SC) one. The transition takes place over a range of doping levels where, at low enough temperatures, the samples are both superconducting and magnetic^{1,2,3}. It is natural to expect phase separation due to the inhomogeneous doping. However local probe such as muon spin relaxation indicates that the magnetic volume fraction is 100%, namely, the magnetic field exists everywhere, even in the SC regions¹. Therefore, the nature of the presence of SC and magnetism is unclear. Are the two orders coupled, and if yes, what are the sign and strength of the coupling? What is the order of the transition between the AFM and SC phases as a function of doping? Is it first order with phase separation or second order with coexistence?

Here we answer this question by looking at the effect of current I on the magnetic phase transition temperature, T_m . A current, on the scale of the second critical current I_{c2} , diminishes the superconducting order parameter. If the two orders interact, the magnetic order parameter is expected to react to the current and either increase or decrease depending on the type of coupling between the two orders. This, in turn, will increase or decrease T_m , respectively. Therefore, we map the magnetic phase transition with and without current. We find that, with current, the magnetic phase transition temperature increases. This results implies that the orders are coupled, and that they are repulsive. Analysis based on the Ginzburg-Landau (GL) model shows that the phase transition is close to the border between first and second order.

The experiment is done with an 8 m long wire made of $\text{La}_{1.94}\text{Sr}_{0.06}\text{CuO}_4$ film. The film is prepared using laser ablation deposition on (100) LaAlO_3 substrate, standard photolithographic patterning and wet acid etching (0.05% HCl). The 6% Sr doping was chosen since the corresponding bulk material has a $T_c \approx 10 \text{ K}$ and

$T_m \approx 6 \text{ K}$ ^{1,4,5}, which makes both critical temperatures reachable in a standard cryostat. The cross section of the wire is $0.5 \times 100 \text{ nm}$ so that a typical applied current of a few mA is comparable to I_{c2} . Probing the magnetic properties of such a thin wire is achieved by using the new low energy muon spin relaxation (LE-SR) technique^{6,7}. In this technique, the muons are first slowed down in an Ar moderator where their kinetic energy drops from 4 MeV to 15 eV, while their initial full polarization is conserved. They are then electrostatically accelerated to 15 keV and transported in ultra high vacuum (UHV) to the sample. Four counters collect positrons from the asymmetric muon decay. One pair of counters is parallel to the initial muon spin direction and the other pair is perpendicular to it. The muon asymmetry in these directions is calculated by taking the difference over the sum of the count for each pair. This asymmetry is proportional to the component of the muon polarization in each direction. The field the muon experience is either internal, below T_m , or external (designated by H), or both. For more details on SR in the presence of superconductivity and magnetism see Ref. 8. The muons beam spot size has a 15 mm diameter (FWHM). In order to avoid muons missing the sample, the wire is folded in the form of a long meandering line covering a disc 3 cm in diameter. The inset of Fig. 1 shows a magnified image of one corner of the sample.

First, we discuss the sample characterization. In order to verify that the wire is indeed a bulk superconductor and that the current flows in the bulk of the wire we performed transverse field LE-SR measurements in a field of $H = 1 \text{ kG}$. Figure 1(a) depicts the results from the magnetic phase ($T = 2.9 \text{ K}$) in a rotating reference frame, using zero field cooling (ZFC). The muons depolarize very quickly and after 3 ns the remaining decay asymmetry is due to muons that have stopped in the substrate. For comparison, data from a blank substrate, normalized by its effective area, are also shown. We also

present the decay asymmetry in the pure superconducting phase ($T = 6\text{ K}$) using field cooling (FC) conditions. In this case, the muon polarization is lost exponentially versus time at a rate r_{sc} due to the magnetic field distribution of the vortices in the superconducting phase. After 6 s the polarization reaches the level of the substrate and the ZFC run, and thus most of the muons are affected by vortices.

We fit the function:

$$A_{sy}(t) = A_{sc} e^{-(r_n t)^2 = 2 r_{sc} t} \cos(\omega_{sc} t) + A_{sb} e^{-r_{sb} t} \cos(\omega_{n sb} t) + A_n e^{-(r_n t)^2 = 2 r_{sc} t} \cos(\omega_{n sb} t)$$

to the muon decay asymmetry at all temperatures. Here A_{sc} , A_{sb} , and A_n represent the respective contributions from the part of the meander that turns superconducting upon cooling, the substrate, and the part of the meander that remains normal upon cooling. r_{sc} , r_{sb} , and r_n are the relaxation rates of muons that land in a superconducting, substrate, and normal material, respectively. $\omega_{n sb}$ is the rotation frequencies in the normal material and the substrate (taken to be equal). ω_{sc} is the rotation frequency in the superconducting part. The only parameters that are allowed to vary with T are r_{sc} and ω_{sc} . The superconducting volume fraction is estimated from $A_{sc} = (A_{sc} + A_n)$ and was found to be $90 \pm 5\%$.

Figure 1(b) shows r_{sc} and the resistivity versus temperature. The midpoint of the resistivity transition to the superconducting state, and the onset of $r_{sc}(T)$ occur at $T_c = 16\text{ K}$. The London penetration depth λ_{ab} at $T = 7\text{ K}$ is 500 nm as estimated from the relation $r_{sc} = 0.04 \lambda_{ab}^2$ where $\lambda_{ab}^2 = 13.5\text{ MHz/kG}$ is the muon gyromagnetic ratio, and λ_{ab} is the magnetic flux quantum⁹. This penetration depth value is similar to the meander thickness and therefore the current will flow uniformly in the bulk of the meandering wire.

It is challenging to flow a current in the meander line during a LE-SR experiment while keeping its temperature well determined. This results from the fact that the sample is cooled by a cold finger in a UHV ambient. Above the first critical current, I_{c1} , the superconducting wire acts as a heater and is not in thermal equilibrium with either the cold finger or any attached thermometer. Therefore, the wire's temperature can be measured only by an a priori calibration procedure. For this, we chose to take the $V-I$ curve of the wire at each temperature in a flow cryostat. In such a cryostat the thermal contact between the wire and a thermometer, even at high currents, is good. Using this calibration, the wire acts as its own thermometer. To account for possible drifts in the calibration we repeated the calibration in the flow cryostat also after the LE-SR experiment. This proved the temperature uncertainty to be smaller than 0.01 K , namely, when we say that we are comparing two runs with equal temperatures we mean that we managed to keep the two runs 0.01 K away from each other.

Fig. 2(a) shows several $V-I$ curves recorded at different temperatures on a short segment (1 cm long) of the wire.

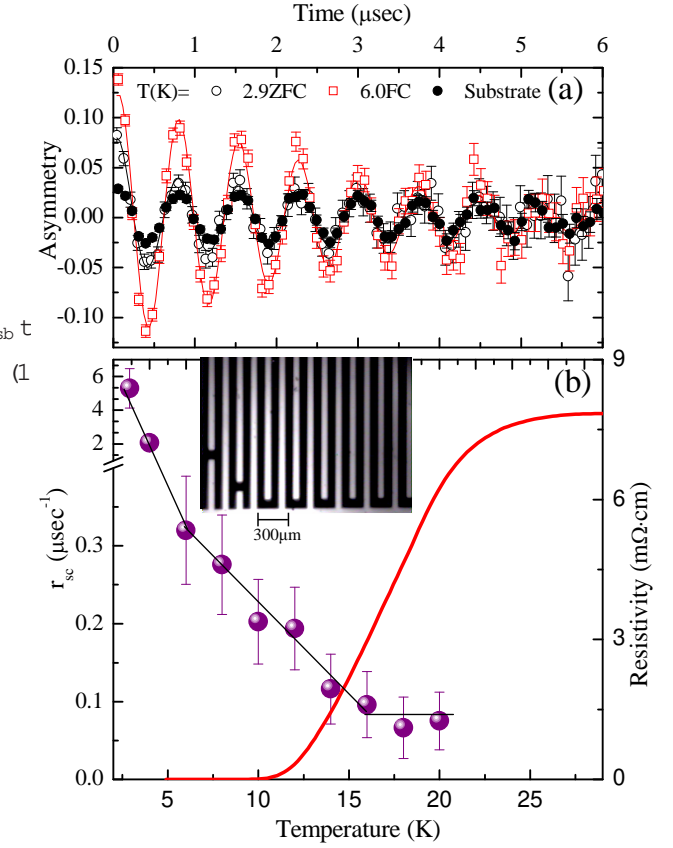


FIG. 1: (color online) Determination of the superconducting volume fraction and penetration depth (a) SR asymmetry under an applied field of 1 kG in a rotating reference frame at $T = 2.9\text{ K}$ with zero field cooling, $T = 6.0\text{ K}$ with field cooling, and at $T = 5\text{ K}$ from the substrate. (b) The resistivity and muon depolarization rate r_{sc} as a function of temperature showing T_c . Below $T_m \approx 6\text{ K}$ the muon relaxation increases rapidly.

These $V-I$ curves are used for the determination of I_{c1} and I_{c2} which are needed for the analysis. The curves are fitted to the function $(I - I_{c1})e^{k(I - I_{c1})}$, where θ is the Heaviside step function. It is seen in Fig. 2(a) that, at $T = 12\text{ K}$, I_{c1} drops to zero and the 1 cm segment of the wire shows ohmic behavior with a normal resistance of $R_n = 60\ \Omega$. We estimate I_{c2} using a variation of the onset criterion¹⁰. The exponential dependence of V on I is extrapolated to the value of I that gives a differential resistance equal to R_n . The obtained values of both critical currents as a function of temperature are plotted in Fig. 2(b).

Next, we study the effect of the current on the magnetic order. Figure 3 shows raw muon decay asymmetry data from the meander wire at several temperatures with no external field and in the laboratory frame. The open symbols represent measurements at low currents (used only for temperature determination) and the solid symbols are measurements at high currents. At $T > T_m$, the asymmetry resembles a Gaussian with relatively slow

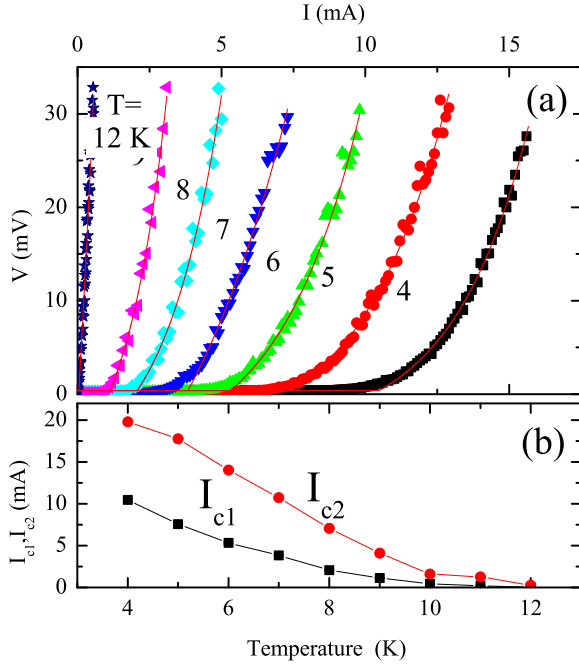


FIG. 2: (color online) Calibration curves used for temperature determination and for the estimation of I_{c1} and I_{c2} . (a) V-I curves of a short segment of the wire. Similar measurements on the full wire are used for the temperature calibration. (b) I_{c1} and I_{c2} as a function of temperature were extracted from the data shown in the top panel.

relaxation, typical of magnetic fields generated by copper nuclear magnetic moments. As the temperature decreases, there is a clear increase in the muon spin depolarization rate indicating that the magnetic order has set in. For comparison, we show in the inset of Fig. 3 standard SR measurements taken with a He flow cryostat on the bulk powder used for making the film. In this case the measurements could be extended to $T = 1.65$ K. We find that the magnetic transition in the wire is very similar to that of ours and others bulk samples^{1,5}, having similar T_m . In addition, the data in the bulk at low enough temperatures is typical of the case where muons in the full sample volume experience frozen magnetism, with spontaneous precession below about 2 K with a frequency $f \sim 3$ MHz, again in agreement with others.

The effect of the current is demonstrated by the $T = 5$ K measurement (red symbols in Fig. 3). The depolarization of the muons spin is faster when a higher current is applied. The difference between the two measurements is emphasized by the shaded area. The change in the asymmetry line shape caused by the application of current is equivalent to cooling by about 0.3 K, although, as mentioned before, the sample temperature is stable to within 0.01 K. This effect was observed at several temperatures along the magnetic transition.

Above T_m and below 4 K the application of current has no effect on the asymmetry. This finding is particularly important since, a priori, the current might affect the

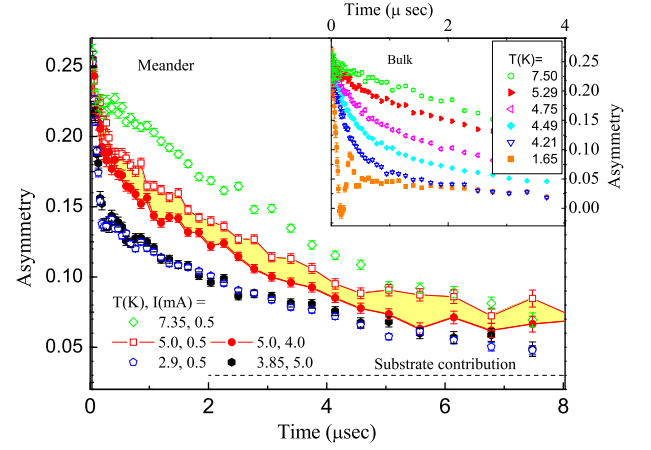


FIG. 3: (color online) Muon decay asymmetry measurements versus time at low current (open symbols) and high current (solid symbols). Different colours represent different temperatures. The area shaded in yellow marks the effect of the current on the muon decay asymmetry at 5 K. The horizontal line shows the expected baseline from the substrate. The inset shows standard SR measurements on the bulk powder used for making the film.

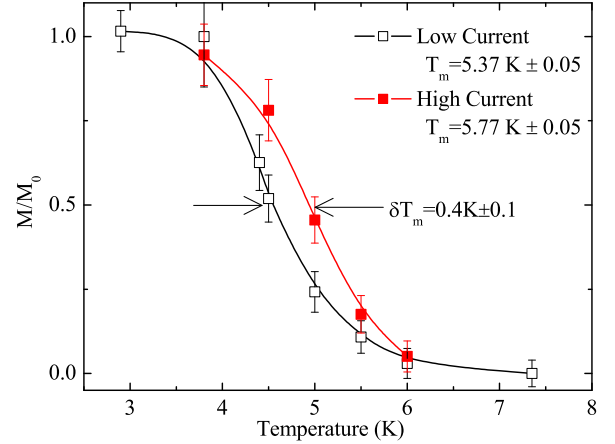


FIG. 4: (color online) The magnetic phase transition, with and without current. Solid lines are guide to the eye.

muon asymmetry directly by means of the magnetic field it produces, or by colliding with the muons. However, we found that once the electronic spins are fully frozen the current does not change the muon asymmetry indicating that there is no direct current muon coupling. This is in agreement with calculations showing that the magnetic field the current produces is very small compared to the internal field. Similarly, the lack of current effect above T_m rules out collisions between muon and electron charge.

In order to determine the magnetic phase transition temperature, without assuming a specific spatial field distribution or temporal fluctuation model, we define the order parameter in a model-free way. At each temper-

ature the asymmetry as a function of time is averaged to produce $\langle \dot{A} \rangle = \frac{1}{t_m} \int_0^{t_m} \dot{A}(t) dt$ where the measurement time $t_m = 8$ sec. We expect $\langle \dot{A} \rangle$ to decrease with increasing magnetic moment size $M(T)$, and therefore defined

$$\frac{M(T)}{M(0)} = \frac{\langle \dot{A} \rangle(T)}{\langle \dot{A} \rangle(0)} = \frac{\langle \dot{A} \rangle(T)}{\langle \dot{A} \rangle(1)} \quad (2)$$

For $\langle \dot{A} \rangle(1)$ we take the averaged \dot{A} at $T = 7.35$ K, which is above the transition. The magnetic phase transition temperature T_m is taken as the onset of the sudden change in $M(T)$. The magnetic transition is sharp enough that other, modelbased, analysis methods gave indistinguishable $M(T)$. The temperature dependence of M with and without current is presented in Fig. 4. We find that the application of a current of about 0.2 J(T) increases the magnetic phase transition temperature by $0.4 - 0.1$ K. This effect means that the two orders interact repulsively. It is complementary to the effect of a strong magnetic field on doped samples, where the magnetic order is enhanced while the superconducting order is suppressed^{11,12}. However, since current, in contrast to magnetic field, does not couple directly to spins, the effect presented here is more simply analyzed. For example, it shows that the enhanced magnetism in the applied field could be a result of supercurrent in the bulk¹³, and not necessarily due to magnetism in the vortex core¹⁴.

A simple interpretation of the result can be given in the framework of the GL model. In this model the free energy density near the critical temperature T_m can be written as $F = a(T) \frac{1}{2} |\psi|^2 + \frac{1}{2} |\mathbf{A}|^2 + U_s |\mathbf{A}|^2 + U_m |\psi|^2 + \frac{1}{2} |\nabla \psi|^2 + \frac{1}{2} |\nabla \mathbf{A}|^2$ (plus gradient terms) where $a(T)$ and $U_s = \frac{2e^2}{v} \frac{T_m}{T}$ are the superconducting and magnetic order parameters respectively, U_{sm} is their coupling constant, v is the unit cell volume, b is a dimensionless parameter, T_m^0 is the magnetic phase transition temperature for $|\mathbf{A}|^2 = 0$, $a(T)$, U_s and U_m are the standard GL parameters. All the parameters can be experimentally determined^{15,16}: $a(T) = \frac{1}{2} \frac{1}{\xi^2} (T - T_m^0)^2$ where $\xi = 2$ nm is the superconducting coherence length¹⁷; $\frac{1}{2} \frac{1}{\lambda^2} = \frac{1}{2} \frac{1}{\lambda^2} = \frac{1}{2} \frac{1}{\lambda^2}$ where $\lambda = 500$ nm is the London penetration depth; $U_s = \frac{1}{2} \frac{1}{\lambda^2}$ according to the minimum condition; $bT_m = \frac{1}{2} \frac{1}{\lambda^2}$ where $\lambda = 4$ nm is the magnetic coherence length^{18,19}; the electron mass can

be approximated by the stiffness of the xy model where $\frac{1}{2} \frac{1}{\lambda^2} = J$, A is the cell area and $J \sim 10^3$ K is the superexchange; from the ratio of muon oscillation frequency between our sample and pure La_2CuO_4 ²⁰ we find a local magnetic moment $M = 0.33 \mu_B$ giving $\frac{1}{2} \frac{1}{\lambda^2} = 0.33^2 v$; $U_m = bT_m = 2 \frac{1}{\lambda^2}$ again by the minimum condition.

U_{sm} is obtained from our current dependent measurement (neglecting gradient terms at this stage). Since T_c is higher than T_m we do not expect $|\mathbf{A}|^2$ to affect $|\mathbf{A}|^2$. Therefore $|\mathbf{A}|^2(T) = |\mathbf{A}|^2(0) (1 - \frac{T}{T_c})^2$. The minimization of F with respect to $|\mathbf{A}|^2$ yields, $|\mathbf{A}|^2 = \frac{b(T_m^0 - T)}{2U_{sm} + U_s}$. Thus, the measured magnetic transition temperature is given by $T_m = T_m^0 - \frac{2U_{sm}}{U_s} \frac{J}{T_m^0}$. We assume that near T_m , $\frac{1}{2} \frac{1}{\lambda^2}(0;T) = \frac{1}{2} \frac{1}{\lambda^2}$ where $\frac{1}{2} \frac{1}{\lambda^2}$ is the ground state value of $\frac{1}{2} \frac{1}{\lambda^2}$. Therefore, the change in the transition temperature, $T_m(T) - T_m(0) = T_m(0) - T_m(T)$, caused by the current is $T_m(T) = T_m(0) - \frac{2U_{sm}}{U_s} \frac{J}{T_m^0}$. The interesting parameter is

$$R = \frac{U_{sm}}{U_s U_m} = \frac{2e^2 M T_m^2 T_m}{U_s J_0 h}$$

where h is the unit cell height. For $R > 1$ the GL model predicts phase separation and first order phase transition. For $R < 1$ the model predicts coexistence and a second order phase transition. The $R = 1$ condition is essential for SO(5) symmetry²¹. At $T = 5$ K we found that $I_{c2} = 17$ mA (see Fig. 2b) and used $I = 4$ mA in the LE-SR. This yields a positive $R = 1.4$. Although numerical factors can change R , they cannot change its proximity to unity.

In summary, we demonstrated the presence of interaction between the magnetic and superconducting order parameters and measured its sign and strength. We find that phase transition at zero temperature from magnetic to superconducting orders, as a consequence of doping, must be very close to the border between first and second order.

We acknowledge very helpful discussions with Assa Auerbach and Yariv Kafri. We also thank the PSI team for supporting the SR experiments, and for providing the continuous high quality beam. This work was also funded in part by the Israeli Science Foundation and the joint German-Israeli DIP project.

¹ Ch. Niedermayer, C. Bernhard, T. Blasius, A. Golnik, A. Moudonbaugh, and J. I. Budnick, Phys. Rev. Lett. 80, 3843, (1998).

² M. H. Julien, F. Borsa, P. Carretta, M. Horvatic, C. Berthier, and C. T. Lin, Phys. Rev. Lett. 83, 604 (1999).

³ J. M. Tranquada et al., Nature 375, 561 (1995).

⁴ C. Panagopoulos, J. L. Tallon, B. D. Rainford, T. Xiang, J. R. Cooper, and C. A. Scott, Phys. Rev. B 66, 064501 (2002).

⁵ B. J. Stemlieb, G. M. Luke, Y. J. Uemura, T. M. Riseman,

J. H. Brewer, P. M. Gehring, K. Yamada, Y. Hidaka, T. Murakami, T. R. Thurston, R. J. Birgeneau, Phys. Rev. B 41, 8866, (1990).

⁶ T. Prokscha, E. Morenzoni, K. Deiters, F. Foroughi, D. George, R. Kobler, A. Suter, V. Vrankovic, Nucl. Instr. Meth. A 595 317-331 (2008).

⁷ E. Morenzoni, F. Kottmann, D. Maden, B. Matthias, M. Meiyberg, T. Prokscha, T. Wutzke, U. Zimmermann, Phys. Rev. Lett. 72, 2793 (1994).

⁸ J. E. Sonier, Reports on Progress in Physics 70, 1717

- (2007).
- ⁹ E. H. Brandt, Phys. Rev. B 37, 2349 (1988).
 - ¹⁰ J. W. Ekin in Concise Encyclopedia of Magnetic and Superconducting Materials, edited by J. E. Evetts (Pergamon, New York, 1991).
 - ¹¹ S. Katano, M. Sato, K. Yamada, T. Suzuki, and T. Fukase Phys. Rev. B 62, R14677 (2000).
 - ¹² B. Lake et al. Nature 415, 299 (2002).
 - ¹³ E. Demler, S. Sachdev, and Y. Zhang, Phys. Rev. Lett 87, 067202 (2001).
 - ¹⁴ Jiang-Ping Hu, Shou-Cheng Zhang, Journal of Physics and Chemistry of Solids 63, 2277 (2002).
 - ¹⁵ K. Huang, Statistical Mechanics 2nd edition, p.425, (John Wiley & Sons, New York, 1987).
 - ¹⁶ P. G. de Gennes, Superconductivity of Metals and Alloys, p.185, (Westview press, 1999).
 - ¹⁷ H. H. Wen, H. P. Yang, S. L. Li, X. H. Zeng, A. A. Soukiassian, W. D. Si and X. X. Xi, Eur. Phys. Lett. 64, 790 (2003).
 - ¹⁸ R. J. Birgeneau et al. Phys. Rev. B 38, 6614 (1988).
 - ¹⁹ B. Keimer et al. Phys. Rev. B 46 14034 (1992).
 - ²⁰ Y. S. Lee et al. Phys. Rev. B 60, 3643 (1999).
 - ²¹ E. Demler, W. Hanke and S. C. Zhang, Rev. Mod. Phys. 76, 909 (2004).